Prabha Materials Science Letters
Vol. 5, No. 1, 174-184, 2026
https://doi.org/10.33889/PMSL.2026.5.1.009

Empirical Modeling and Multi-Objective Optimization of Laser Kerf Geometry in Aluminium Sheets using Response Surface Methodology and ANOVA

Angshuman Roy
Power Engineering Department,
Jadavpur University, Kolkata, 700106, West Bengal, India.
E-mail: angshuman_roy01@yahoo.co.in

Ananta Dutta
Department of Mechanical Engineering,
C.V. Raman Global University, Bhubaneswar, 752054, Odisha, India.
E-mail: ananta.dutta@cgu-odisha.ac.in

Arka Ghosh
Department of Mechanical Engineering,
C.V. Raman Global University, Bhubaneswar, 752054, Odisha, India.
E-mail: arkaiaf@gmail.com

Nikhil Kumar
WMG, The University of Warwick,
Coventry CV4 7AL, United Kingdom.
E-mail: nikhilju2013@gmail.com

Santanu Das
Mechanical Engineering Department,
Kalyani Government Engineering College, Kalyani, 741235, West Bengal, India.
E-mail: sdas.me@gmail.com

Pankaj Shrivastava
Department of Mechanical, Bioresources, and Biomedical Engineering,
College of Science, Engineering and Technology,
University of South Africa, Johannesburg, 1709, South Africa.
Corresponding author: pankaj.62shrivastava@gmail.com

Velaphi Msomi
Department of Mechanical, Bioresources and Biomedical Engineering,
College of Science, Engineering and Technology,
University of South Africa (UNISA), Johannesburg, 1709, South Africa.
E-mail: msomiv@unisa.ac.za

(Received on November 10, 2025; Revised on February 5, 2026 & February 16, 2026; Accepted on February 18, 2026)

Abstract
Laser-based kerfing has been recognized as a potential machining process, considering its non-contact characteristics, precision, and versatility. In this study, an Nd: YVO4 laser with a wavelength of 1064 nm will be employed to study the kerfing process on Aluminium sheets. The main factors considered in the laser kerfing process include power, pulse frequency, and scanning velocity; effects on kerf width will be considered. The results will be presented by considering factors such as kerf width and depth. The experiments will be designed using the Response Surface Methodology, and response surfaces will be developed to study the

interactions between factors and predict results. The study will also include a multi-objective optimization process, considering a minimum kerf width and a maximum kerf depth. Analysis of Variance will be applied to test the significance of factors considered in this study. It is found that the developed response surfaces have significant predictive capability. This study aims to contribute towards an accurate and sustainable laser-based kerfing process on Aluminium-based materials.

Keywords- Aluminium sheets, Nd: YVO_4 laser, Kerf geometry, Response surface methodology (RSM), Multi-objective optimization, ANOVA.

1. Introduction

Lasers are widely used in material cutting and welding, and they also show high efficiency in material kerf removal because of their unique advantages over traditional techniques. This process is flexible, environmentally friendly, and does not depend on the particular properties of the work material. Laser kerf allows product identification through barcodes, logos, numerical values, and other graphical information. This involves melting and vaporizing unwanted matter from the base to generate a focused laser beam with a small spot for high resolution. Various types of lasers have been developed, including those for engraving (Roy et al., 2018; Alhawsawi et al., 2023; Shao et al., 2024; Tian et al., 2025). Tian et al. (2025) investigated the laser processing technique for the development of stable polychrome marking on glass using a brass alloy donor in the back laser-induced film transfer technique. The study emphasized the significance of Cu and Zn oxides in colour generation and the feasibility of developing detailed coloured QR codes. In the study of Qi et al. (2003), the laser engraving of stainless steel using a Q-switched Nd: YAG laser was investigated, indicating that the frequency of the pulses is important for the engraving of the metal in terms of depth and width. Chen et al. (2009) also performed an experiment on the laser marking of eggshells using a 100 W CO2 laser (6 mm beam size, 1 kHz PRF). Genna et al. (2010) performed an experiment on the laser engraving of C45 steel using a 20 W Q-switched Yb: YAG fiber laser at 1070 nm. Leone et al. (2010) aimed at establishing the correlation between various parameters and the engraved marks. The authors found that to obtain satisfactory mark visibility, low frequency and moderate average power should be applied. Peter et al. (2013) have investigated the process of laser engraving on Aluminium and alumina ceramic materials using a CNC-operated Nd: YAG laser. They have used a lens with a focal length of 50 mm, resulting in a spot size of 0.1 mm on the workpiece. Kasman (2013) has investigated machinability on a hard metal, a powder metallurgy material known as Vanadis 10, along with the influence of laser engraving parameters on surface roughness and engraving depth. The author developed a predictive model. Penide et al. (2015) investigate alumina marking using lasers at 1064 nm and 532 nm, focusing on colorimetric contrast, optimal parameters, and the impact of atmospheric conditions, with inert atmospheres producing the darkest marks. Chen et al. (2009) investigated the use of a CO_2 laser marking system for coding Arabic numerals on eggshells. SEM analysis is employed to evaluate marking quality and depth, demonstrating that the method does not damage the eggshell's inner layers or affect the egg theca. Previous RSM/ANOVA-based studies have largely focused on non-reflective or low-reflectivity materials and have primarily reported generic process optimization using CO_2 or fiber lasers. In contrast, investigations on Aluminium commonly rely on empirical models that do not explicitly account for reflectivity-governed laser energy absorption. Moreover, Nd: YVO_4-specific statistical models for laser marking of Aluminium are scarcely reported in the open literature.

This study presents the development of material- and laser-specific RSM models for Nd: YVO_4 laser kerfing of Aluminium sheets, addressing a clear gap in existing statistical modeling research, which has largely focused on CO_2 and fiber lasers. Reflectivity-driven energy coupling effects are inherently incorporated into the RSM–ANOVA framework through statistically significant interaction terms, enabling more accurate and physically meaningful predictions of marking responses on highly reflective Aluminium

surfaces. The study further explains and defines the major interactions among process variables that are unique to Nd: YVO_4 laser kerfing and cannot be addressed by the conventional empirical optimization approach. On the basis of these findings, the study develops a predictive and physically informed optimization approach aimed at improving process robustness and kerf quality. Specifically, the goal is to maximize kerf depth and minimize kerf width. The major process variables, laser power, pulse frequency, and scanning speed, are chosen based on process needs. Single- and multi-objective optimizations of kerf width and depth are performed using Minitab 16, leveraging empirical data obtained from a design of experiments framework and response surface analysis. ANOVA is used to evaluate the relative contribution of individual process variables and their interactions, thus offering a comprehensive and robust optimization strategy for the laser kerf on reflective metal substrates.

Experimental procedure

Laser kerf operation is conducted in this experimental work. Samples of 1.2 mm thickness are first cut to the dimensions of 10 mm × 30 mm, and the work materials are cleaned with acetone to make them oil-free. The Nd: YVO4 laser system was prepared for the kerfing of the prepared specimens. Subsequently, aluminum samples were kerfed using different combinations of process parameters such as laser power, pulse frequency, and scanning speed.

Figure 1. Photographic view of a kerf sample.

A typical kerfed specimen is shown in **Figure 1**. Observation and measurement of the depth and width of kerfing grooves are made using an optical microscope (make: Leica, model: Leica L2). The experiment is carried out using five levels of each of three factors. Experiments are planned using a DOE using RSM. The total number of experimental runs is 20, and the data obtained are entered into Minitab 16 for further processing.

Pilot Diode Laser system (Make: Electrox) used is of wavelength of 635-680 nm, maximum power of 1 mW with CW (continuous type) output. Working Laser is of Nd: YVO_4 (Neodymium-doped Yttrium Orthovanadate) having 12 W power, frequency range of 0 to 500 kHz, kerfing speed of 0.15 to 10160 mm/s, wavelength of 1064 nm (nano meter) and Galvo lens (S163). Under 50X magnification, the kerf width and depth are examined.

2. Results and Discussion

The measured value of responses and the actual value of the experimental design matrix are shown in **Table 1**. Laser kerfing is done along a straight line on an Aluminium sheet with different process parameter combinations. For observing kerf depth and width, samples are cold-mounted. After solidification, specimens are polished by a velvet cloth polishing machine with the help of diamond paste. The depth and width of the kerf were measured using an optical microscope. **Figure 2(a)** and **2(b)** illustrate the kerf width and depth.

This study aims to use RSM and Mathematical Modelling to evaluate the effects of Laser Power (P), Scanning Speed (S), and Pulse Frequency (f) on the kerf width and depth. Equation (1) is the general form of the quadratic model, which is a second-degree polynomial.

$$y = \beta_0 + \sum_{i=1}^{k} \beta_i x_i + \sum\sum \beta_{ij} x_i x_j + \sum_{i=1}^{k} \beta_{ii} x_i^2 + \varepsilon \quad (1)$$

where, $\beta_0, \beta_i, \beta_{ij}, \beta_{ii}$ denotes regression coefficient for I = 0, 1,....., k *and* j = 0, 1,...., k.

The regression coefficients are represented by $\beta_0, \beta_i, \beta_{ij}$, and β_{ii}, where the indices I = 0, 1, ..., k and j = 0, 1, ..., k.

From regression analysis on experimental data, expressions for kerf width (MW) and kerf depth (MD) are evaluated as shown in Equations (2) and (3).

MW = -24.6 + 1.48 P – 1.51 f + 0.21 s – 0.00943 P×P + 0.0480f×f – 0.0412S×S – 0.0065 P×f + 0.0142 P×S – 0.0196 f×S (μm) (2)

MD = 258.213 – 2.83 P – 1.67 f – 14.16 S + 0.0093 P×P + 0.2002 f×f + 0.084 S×S – 0.0746 P×f + 0.0815 P×S + 0.213 f×S (μm) (3)

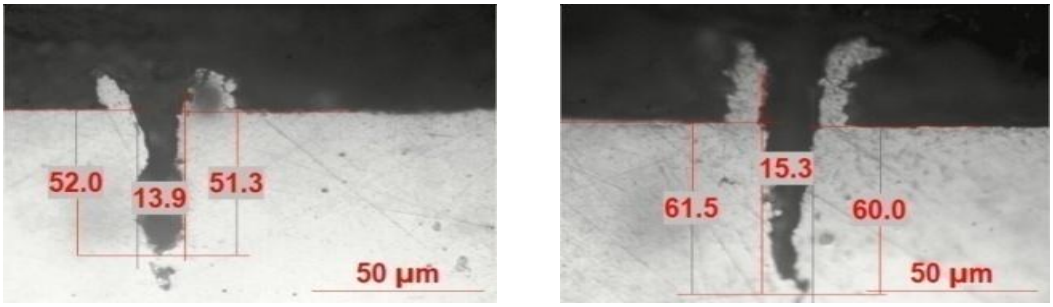

(a) (b)

Figure 2. (a, b) Kerf specimen's measurements of width as well as depth under various parametric conditions.

Table 1. Actual values, experimental design matrix, and the measured responses.

Power (W)	Frequency (kHz)	Scanning speed (mm/s)	Kerf width (μm)	Kerf depth (μm)
9.00	14.00	23.40	12.81	45.25
7.80	20.00	10.00	15.30	60.75
7.80	8.00	10.00	23.04	54.51
9.00	14.00	15.00	16.43	55.25
10.92	14.00	15.00	21.11	75.15
9.00	14.00	15.00	24.63	69.85
9.00	14.00	15.00	18.81	49.35
9.00	3.90	15.00	38.82	17.09
10.20	8.00	20.00	28.04	26.29
7.80	8.00	20.00	24.01	24.43
9.00	24.09	15.00	15.32	63.22
7.80	20.00	20.00	11.04	24.66
6.96	14.00	15.00	13.90	51.65
10.20	8.00	10.00	27.11	71.71
9.00	14.00	6.59	21.07	88.49
9.00	14.00	15.00	18.00	44.31
9.00	14.00	15.00	21.72	58.90
10.20	20.00	10.00	15.31	64.19
9.00	14.00	15.00	22.42	63.83
10.20	20.00	20.00	16.04	76.05

A. Parametric evaluation of laser kerfing characteristics

***Kerf width*:** This article seeks to explore the influence of width variation on Nd:YVO4 using parametric effects. The width of the kerf is also analyzed using response surface plots. A mathematical model for the width of the kerf is developed using Equation (2). As seen in **Figures 3(a)** and **3(b)**, the conventional three-dimensional representations of the width of the kerf, **Figure 3(a)** shows the surface relationship for the width of the laser-kerf, input power, and scanning speed, while the frequency of the pulses is kept constant at 24.09 kHz. The width of the kerf increases with the input power and speed, then starts to decrease. However, if the frequency of the pulses is increased while the input speed is kept constant at 15 mm/s, the width of the kerf starts to decrease, then increases.

It is postulated that, as the frequency increases, the maximum power that can be achieved may reduce, perhaps not being sufficient to vaporize the considerable amount of material. Thus, some of the material may remain molten. Hence, the width of the marks produced is expected to reduce with increasing pulse frequencies. The kerf width is expected to increase with increasing power, but an increasing pulse frequency is expected to produce the reverse effect. Furthermore, an increase in scanning speed may reduce the power, perhaps not being sufficient to vaporize the material. The breadth of the kerf is also influenced by the size of the concentrated point. As the pulse frequency increases, the spot size shrinks, resulting in more precise kerfing. The diverse nature of distinct parameters requires the use of an optimization tool to get an appropriate combination of parameters that provides the desired outcome.

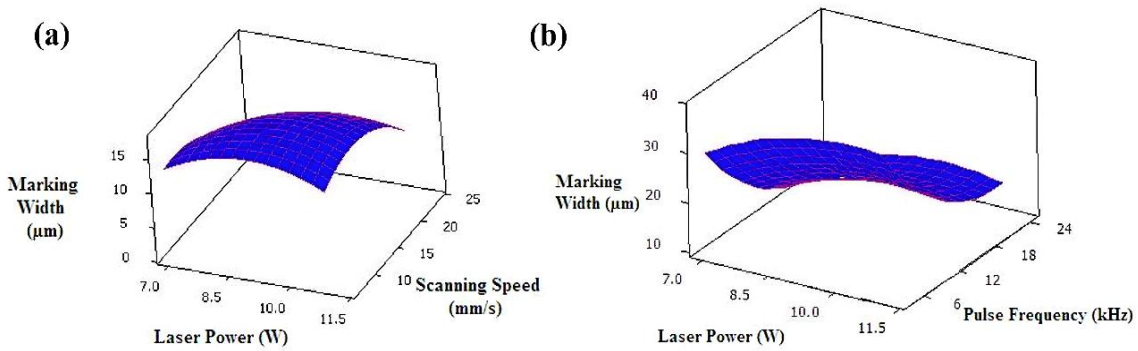

Figure 3. Response surfaces for (a) laser power versus scanning speed on kerf width at 24.09 kHz and (b) laser power versus pulse frequency on kerf width at 15 mm/s.

***Kerf depth*:** The effect of kerf depth with respect to increased power, scanning speeds, and frequency of the laser pulse is depicted in **Figure 4(a, b)**. It was previously discussed that increasing power increases the energy that is absorbed by the laser beam, thus increasing its penetration depth, as depicted in **Figure 4(a, b)**. The depth increases with an increase in frequency and a decrease in scanning speeds.

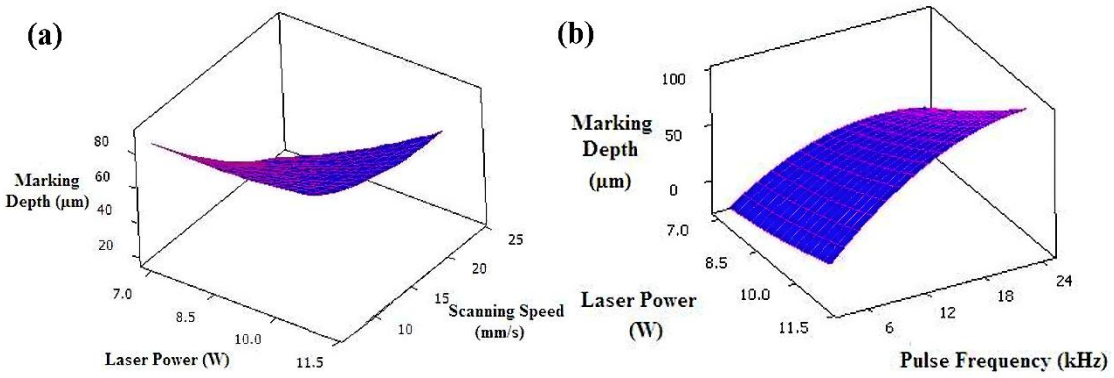

Figure 4. Response Surface: Combined effect of laser power and scanning speed on the kerf depth at 14 kHz frequency, and (b) power and pulse frequency on the kerf depth at 23.41 mm/s scanning speed.

B. Parametric optimization for minimization of kerf width

The response surface tool in Minitab 16 software is used to pick the best process settings to achieve the required kerf with the smallest kerf width.

Table 2. ANOVA for kerf width.

Source	DF	Seq SS	Adj SS	Adj MS	F	P
Regression	9	719.253	719.253	79.917	10.53	0.001
Linear	3	582.219	39.761	13.254	1.75	0.221
P	1	47.519	17.455	17.455	2.30	0.160
f	1	517.059	14.332	14.332	1.89	0.199
S	1	17.641	1.314	1.314	0.17	0.686
Square	3	129.091	129.091	43.030	5.67	0.016
P*P	1	20.433	17.505	17.505	2.31	0.160
f*f	1	83.836	74.382	74.382	9.80	0.011
S*S	1	24.823	24.823	24.823	3.27	0.101
Interaction	3	7.942	7.942	2.647	0.35	0.791
P*f	1	1.194	1.194	1.194	0.16	0.700
P*S	1	3.063	3.063	3.063	0.40	0.540
f*S	1	3.686	3.686	3.686	0.49	0.502
Residual Error	10	75.887	75.887	7.589		
Lack-of-Fit	5	28.148	28.148	5.630	0.59	0.712
Pure Error	5	47.739	47.739	9.548		
Total	19	795.140				

The analysis of variance test is applied to determine if there is a significant effect on the width of the kerf due to the parameter of laser kerfing. The result of the test is shown in **Table 2** above.

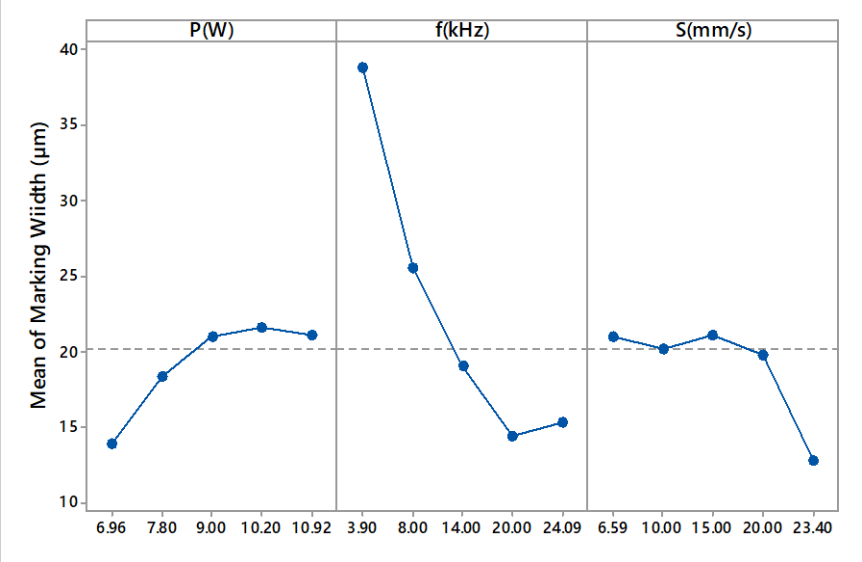

Figure 5. The plot shows the main effects of kerf width, using laser power, scanning speed, and pulse frequency.

Table 3. Analysis of variance (ANOVA) for kerf depth.

Source	DF	Seq SS (Sequential sum of squares)	Adj SS (Adjusted sum of squares)	Adj MS (Adjusted mean square)	F	P
Regression	9	5819.78	5819.78	646.643	5.03	0.009
Linear	3	4273.99	490.82	163.605	1.27	0.336
P	1	928.51	49.92	49.917	0.39	0.547
f	1	1167.87	8.87	8.866	0.07	0.798
S	1	2177.61	488.00	487.998	3.79	0.080
Square	3	924.36	924.36	308.119	2.39	0.129
P×P	1	31.48	15.39	15.388	0.12	0.737
f×f	1	828.49	776.17	776.167	6.03	0.034
S×S	1	64.39	64.39	64.385	0.50	0.496
Interaction	3	621.44	621.44	207.147	1.61	0.248
P×f	1	159.94	159.94	159.937	1.24	0.291
P×S	1	132.93	132.93	132.927	1.03	0.333
f×S	1	328.58	328.58	328.577	2.55	0.141
Residual Error	10	1286.84	1286.84	128.684		
Lack-of-Fit	5	848.88	848.88	169.776	1.94	0.243
Pure Error	5	437.96	437.96	87.592		
Total	19	7106.62				

The relative importance of the parameters is further determined by performing an ANOVA test at a confidence level of 95%. The result of the test on the width of the kerf is shown in **Table 2** above, along with some explanations on some of the statistical terms used in the table. DF denotes degrees of freedom, SS: sum of squares, MS: mean square, F: Fisher's ratio, and P: probability of significance. From the table, we see that P, which stands for "probability of significance," is less than 0.05 for power and the square of frequency.

In the current study, the ANOVA output shows that the f^2 term is a significant factor affecting the kerf width. In terms of depth, the analysis also shows that the f^2 term is the most important factor, consistent with the corresponding P-values. The R^2 and adjusted R^2 values are also presented to demonstrate the

goodness of fit. Therefore, these factors are very important in the determination of kerf width during laser kerfing processes. The optimal process parameters that minimize the width are determined to be 6.96 W of laser power, 20 kHz of pulse frequency, and 23.409 mm/s of scanning speed (**Figure 5**). The single-objective optimum solution for kerf width is 6.96 W / 20 kHz / 23.4 mm/s, and the multi-objective optimum solution for kerf width and depth is 10.92 W / 24.09 kHz / 23.4 mm/s. This is a compromise solution where the kerf width is slightly increased while the depth is maximized. The results can be interpreted based on the laser energy density, pulse overlap, and aluminium reflectivity. Increasing the energy density increases the depth, but high pulse overlap leads to wider kerf width due to thermal accumulation, and high reflectivity reduces the energy absorption. The multi-objective optimum solution of 10.92 W / 24.09 kHz / 23.4 mm/s is consistent with the results of a previous study on aluminium, showing the trade-off between kerf width and depth, and the need to include material-specific optical effects in the optimization process.

C. Parametric optimization for maximization of kerf depth

The other desired outcome is to attain the highest kerf depth possible. Analysis of experimental data is carried out using ANOVA to determine the important factors affecting kerf depth, with 95% confidence intervals. **Table 3** presents the ANOVA results for kerf depth. From the results, it is clear that the P-values of power, frequency, scanning speed, and the square of the frequency are less than 0.05, which means that all these parameters have significant effects on kerf depth in the laser kerfing process. The optimal combination of process variables, which can give the minimum kerf depth, is achieved by using 91.82% of 12 W of laser power, 24.0908 kHz of frequency, and 23.409 mm/s of scanning speed, as shown in **Figure 6**.

D. Multi-objective optimization

The numerical optimisation approach of Minitab 16 software is used to perform multi-objective optimisation of kerf width and depth during laser kerfing on aluminium. The result of the multi-objective optimisation system is shown in **Figure 7**. Here, the aim is to find the optimum process parameters that can achieve the minimum width while maximizing the depth of the kerf. The optimum process parameters of the laser power, speed of scanning, and frequency of pulses are determined to be 10.92 W, 23.409 mm/s, and 24.0908 kHz, respectively.

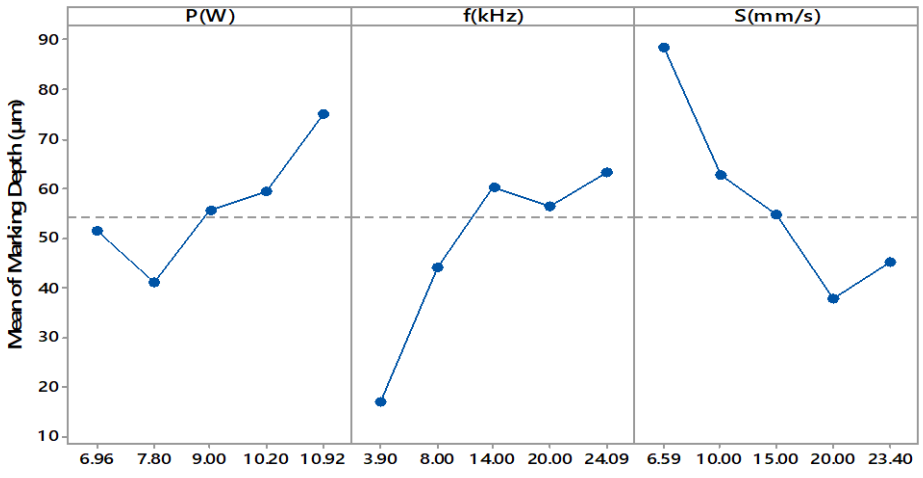

Figure 6. The plot shows the main effects of kerf depth, using laser power, scanning speed, and pulse frequency.

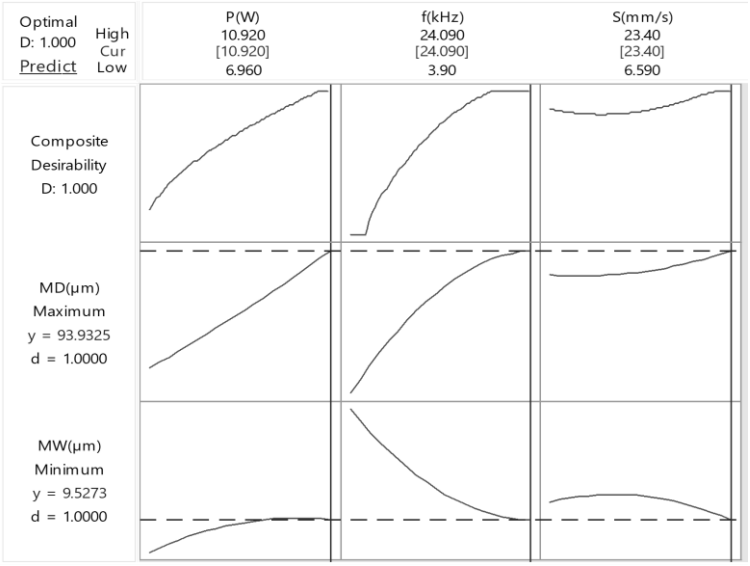

Figure 7. Variation of kerf depth and width based on laser power, pulse frequency, and scanning speed.

E. Reflectivity test

This study also assesses the reflectivity of aluminium specimens to determine the reduction in reflectivity caused by aluminium kerfing. The test was conducted using a Spectro Photometer with the Perkin Elmer UV Win lab Data Processor and Viewer Version 1.00. The reflectivity of the aluminium sheet at the kerfing position, measured at a wavelength of 1064 nm, is about 26% as seen in **Figure 8**.

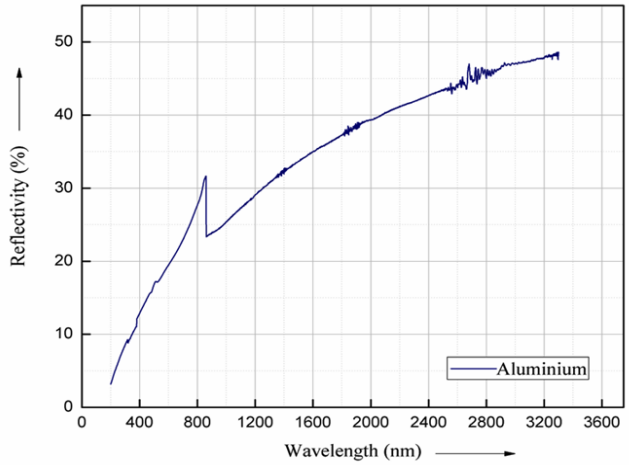

Figure 8. Variation of reflectivity of Aluminium sheet with its wavelength.

3. Conclusions

This work offers a statistical framework for Nd: YVO_4 laser marking of Aluminium sheets that is particular to both material and laser. The suggested method integrates reflectivity-driven energy absorption through statistically significant parameter interactions, in contrast to earlier RSM/ANOVA-based studies that only rely on empirical optimization. This allows for more precise and physically significant predictions. The

proposed models give a strong foundation for industrial laser kerfing of reflective metallic materials, as well as improved predictive capability and useful suggestions for process optimization. In order to investigate the effects of important process factors on the kerfing process, this experimental investigation uses an Nd: YVO_4 laser operating at a wavelength of 1064 nm to execute kerfing on Aluminium plates with a thickness of 1.2 mm. The results increase the applicability of statistical modelling methods to application-focused, physically informed laser-material interaction studies. Based on the findings, a few conclusions may be drawn.

- Increasing the pulse frequency will reduce the width of the kerf. Increasing the laser speed will also reduce the width of the kerf slightly, while decreasing the pulse frequency will increase the width of the kerf more. Increasing the laser power will also increase the width of the kerf.
- Increasing the laser power will increase the depth of the kerf, while increasing the laser speed will reduce the depth of the kerf slightly.
- The analysis of variance shows that the process parameters of power, along with the square of the frequency, have the most significant effect on kerfing width, along with power, pulse frequency, and scanning speed. The most significant variable for kerf depth is the square of the frequency.
- The optimum conditions for achieving the maximum kerf depth with minimum kerf width are 10.92 W of power, 24.0908 kHz of frequency, and 23.409 mm/s of scanning speed.

Conflicts of Interest

The authors confirm that there is no conflict of interest to declare for this publication.

Acknowledgments

This study did not receive specific funding from public, commercial, or not-for-profit agencies. The authors thank the editor and anonymous reviewers for their helpful comments.

AI Disclosure

The author(s) declare that no assistance is taken from generative AI to write this article.

References

Alhawsawi, A.M., Moustafa, E.B., Fujii, M., Banoqitah, E.M., & Elsheikh, A. (2023). Kerf characteristics during CO2 laser cutting of polymeric materials: experimental investigation and machine learning-based prediction. *Engineering Science and Technology, an International Journal*, *46*, 101519.

Chen, M.F., Hsiao, W.T., Huang, W.L., Hu, C.W., & Chen, Y.P. (2009). Laser coding on the eggshell using pulsed-laser marking system. *Journal of Materials Processing Technology*, *209*(2), 737-744.

Chen, M.F., Hsiao, W.T., Huang, W.L., Hu, C.W., & Chen, Y.P. (2009). Laser coding on the eggshell using pulsed-laser marking system. *Journal of Materials Processing Technology*, *209*(2), 737-744.

Genna, S., Leone, C., Lopresto, V., Santo, L., & Trovalusci, F. (2010). Study of fibre laser machining of C45 steel: influence of process parameters on material removal rate and roughness. *International Journal of Material Forming*, *3*, 1115-1118.

Kasman, Ş. (2013). Impact of parameters on the process response: a Taguchi orthogonal analysis for laser engraving. *Measurement*, *46*(8), 2577-2584.

Leone, C., Genna, S., Caprino, G., & De Iorio, I. (2010). AISI 304 stainless steel marking by a Q-switched diode pumped Nd: YAG laser. *Journal of Materials Processing Technology*, *210*(10), 1297-1303.

Penide, J., Quintero, F., Riveiro, A., Fernández, A., Del Val, J., Comesaña, R., Lusquiños, F., & Pou, J. (2015). High contrast laser marking of alumina. *Applied Surface Science*, *336*, 118-128.

Peter, J., Doloi, B., & Bhattacharyya, B. (2013). Analysis on the characteristics of Nd: YAG laser marking on alumina ceramic based on RSM. *International Journal of Materials and Product Technology*, *46*(1), 2-18.

Qi, J., Wang, K.L., & Zhu, Y.M. (2003). A study on the laser marking process of stainless steel. *Journal of Materials Processing Technology*, *139*(1-3), 273-276.

Roy, A., Kumar, N., Das, S., & Bandyopadhyay, A. (2018). Optimization of pulsed Nd: YVO4 laser marking of AISI 304 stainless steel using response surface methodology. *Materials Today: Proceedings*, *5*(2), 5244-5253.

Shao, J., Liang, X., Lin, Y., Shen, Q., Ren, J., & Han, J. (2024). Excimer laser marking− A precise patterning technique for material surfaces. *Optics & Laser Technology*, *176*, 110974.

Tian, Y., Zhang, W., Wang, Y., Zhang, Y., Hou, X., & Li, Y. (2025). Generating readable two-dimensional codes on denim fabric using laser marking. *Optics & Laser Technology*, *183*, 112272.